Supporting Information

# Active-Powering Pressure-Sensing Fabric Devices

Hongyan Sun,[a] Ning Pan,[b] Xin Jin,[a] Ka Deng,[a] Zhiduo Liu,[c] Cheng-Te Lin,[d] Tingrui Pan*[b] and Yu Chang*[a]

a. Bionic Sensing and Intelligence Center (BSIC), Institute of Biomedical and Health Engineering, Shenzhen Institutes of Advanced Technology, Chinese Academy of Science, 1068 Xueyuan Avenue, Shenzhen 518055, China. E-mail: yu.chang@siat.ac.cn
b. Micro-Nano Innovations (MINI) Laboratory, Department of Biomedical Engineering, University of California Davis, One Shields Avenue, Davis, CA 95616, USA.
c. University of Chinese Academy of Sciences, 19 A Yuquan Rd., Shijingshan District, Beijing, 100049, China.
d. Key Laboratory of Marine Materials and Related Technologies, Zhejiang Key Laboratory of Marine Materials and Protective Technologies, Ningbo Institute of Materials Technology and Engineering, Chinese Academy of Sciences, Ningbo, 315201, China.

**Figure S1-S7, Table S1, Video S1-S2.**

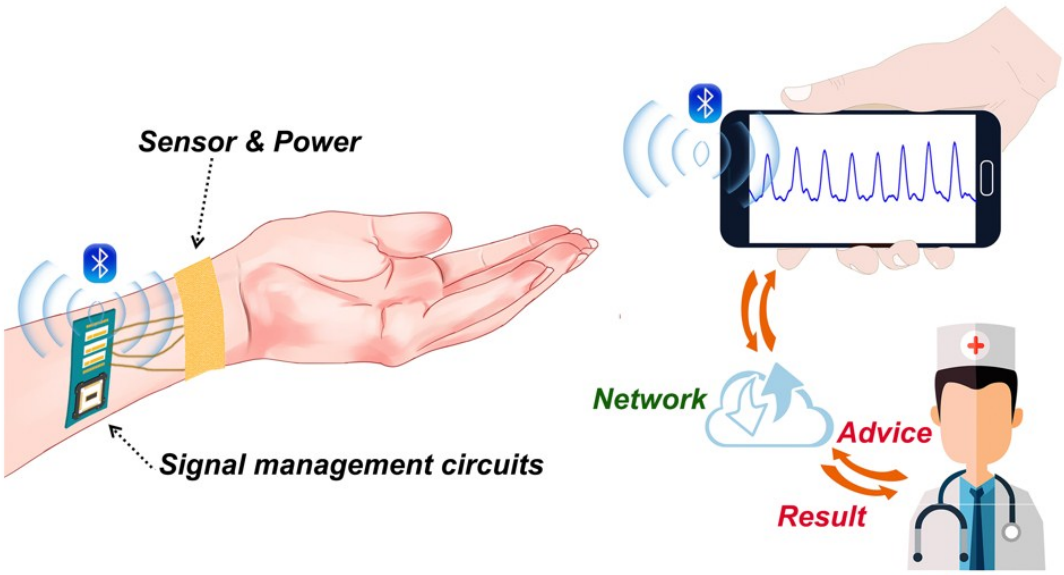


**Figure S1**. Potential application of the APPS fabric device for wearable physiological monitoring.

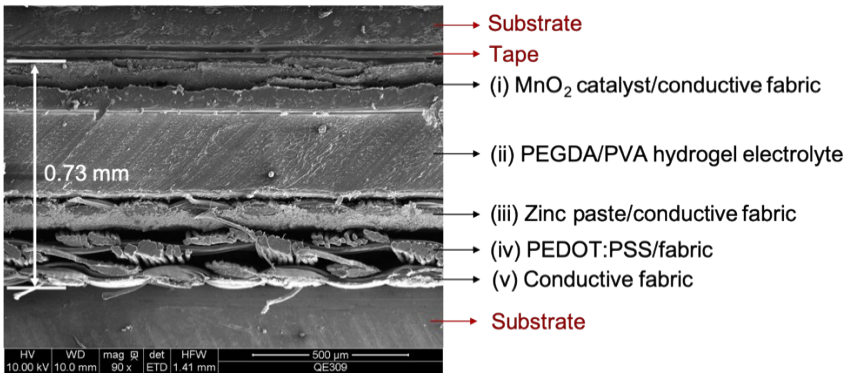


**Figure S2.** The SEM of cross-section of the APPS fabric

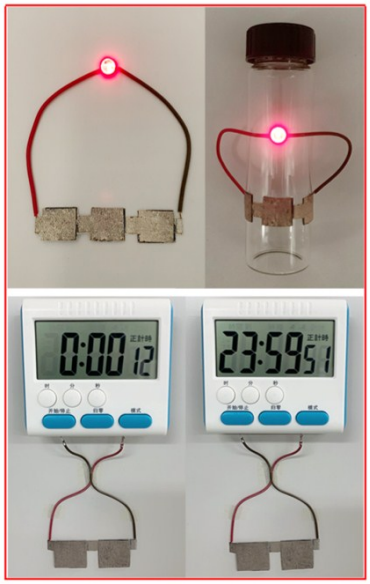

**Figure S3**. Driving LED and electronic watch.

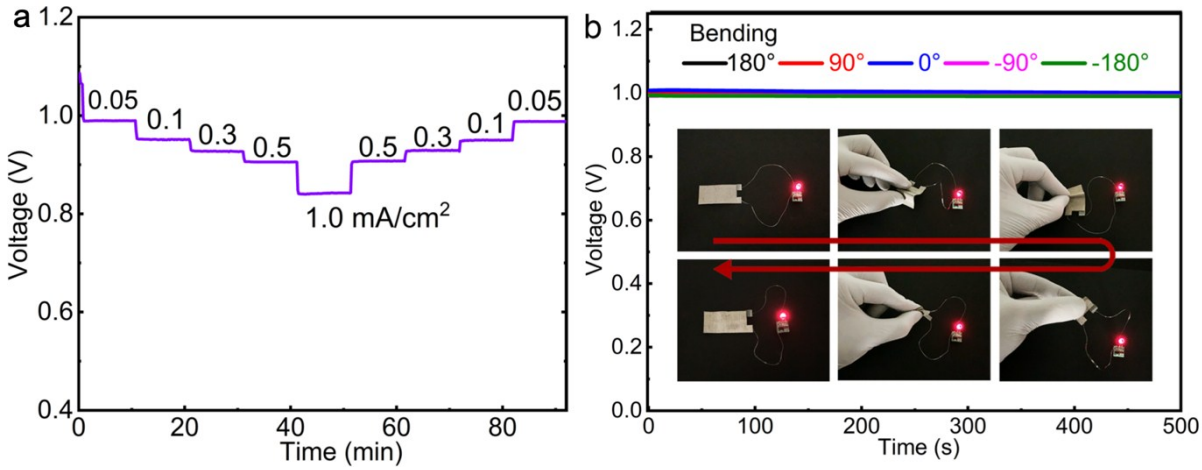


**Figure S4**. a) Discharge curves at different current densities. b) Discharge curves of the device with different bending angles and the stability.

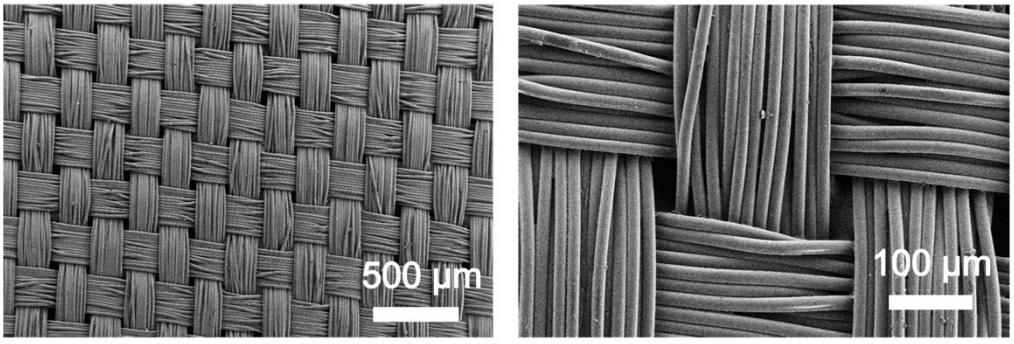


**Figure S5.** SEM image of the PEDOT:PSS/fabric.

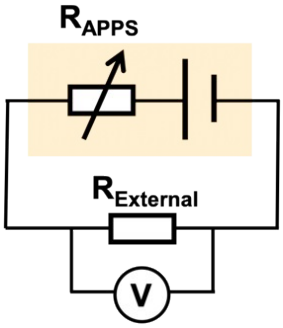


**Figure S6.** The voltage change ($V-V_0$) according to the equivalent circuit and was recorded by a data acquisition card.

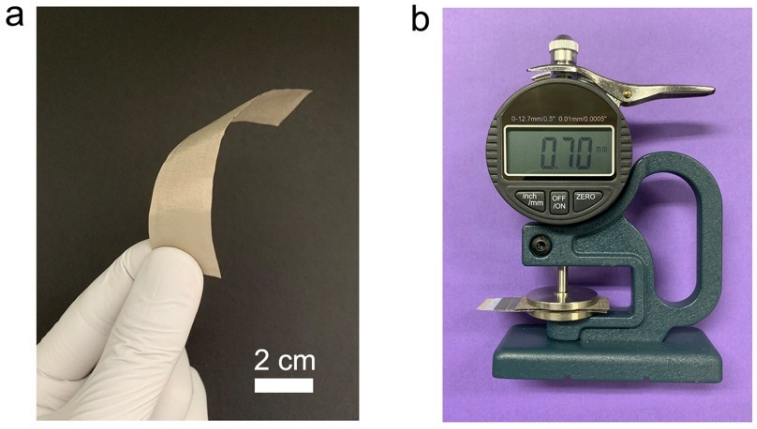


**Figure S7.** A photograph of a) the APPS fabric and b) the thickness.

**Table S1.** Comparison of the key parameters of our active-powering pressure sensor and recently reported flexible pressure sensors for wearable physiological and activity monitoring.

| Transduction mechanisms | Materials | Maximum detection pressure [kPa] | Detection limit [Pa] | Response time [ms] | Reference |
|---|---|---|---|---|---|
| Piezoresistive | Graphene/PDMS | 40 | 1.8 | 0.5 | Nano Energy, 2019, 59, 422-433. |
| Piezoresistive | rGO/PDMS | 40 | 16 | 120 | ACS Nano, 2018, 12, 2346-2354. |
| Piezoresistive | PEDOT:PSS/AgNWs | 90 | 20 | 60 | Adv. Mater. Technol. 2019, 1800640. |
| Piezoresistive | Carbon black | 16.4 | 91 | 20 | Adv. Funct. Mater. 2016, 26, 6246. |
| Iontronic | Epidermal-iontronic interface | 30 | 800 | NA | Adv. Mater. 2018, 1705122. |
| Iontronic | Iontronic paper | 25 | 6.2 | 5 | Adv. Funct. Mater. 2019, 1807343. |
| Capacitive | Natural Plant | 115 | 0.6 | NA | Small 2018, 1801657. |
| Piezoelectric | FEP/f-PTFE | 30 | 5 | 500 | Nano Energy, 2017, 32, 42-49. |
| Triboelectric | FEP nanorod arrays | ~13 | 0.16 | NA | Adv. Funct. Mater. 2014, 24, 5807-5813. |
| Triboelectric | Gelatin nanofiber | ~25 | ~0.3 k | NA | Nano Energy, |

| | | | | | |
|---|---|---|---|---|---|
| | | | | | 2017, 36, 166-175. |
| Triboelectric | PTFE | 1.3 | 2.5 | 5 | Adv. Funct. Mater. 2019, 29, 1806388. |
| Piezoresistive | PEDOT:PSS/fabric | > 300 | 42.6 | 9 | This work |

**Video S1.** The video of arterial pulse waveforms can be apparently observed and wireless data transmission to personal computer.

**Video S2.** The real-time pressure pulse waveforms had been converted into the modulation of the light intensity in LED.

**Mathematical Derivations for the Mechanical-to-Capacitance behavior**

The mechanical deformation of a fabric can be predicted using the classical compression behavior of fibrous assembly [1]. When a pressure $P$ is applied to the fibrous assembly, the relationship between the pressure and the volume of the assembly is

$$P = \lambda\left(\frac{1}{v^3} - \frac{1}{v_0^3}\right), \quad [1] \qquad (1)$$

where $v$ is the volume of the assembly, and $v_0$ is the volume of the assembly when $P = 0$. $\lambda = KEm^3\rho^{-3}$, the constant $K$ represents the spatial distribution and other characteristics of the fibers, and is related to force distribution on fibers and derived from the bending formula of simply supported beam [2]. $E$, $m$ and $\rho$ are respectively the fiber tensile modulus, the mass and density of the assembly [2].

As the relationship between fiber volume fraction ($V_f$) and volume of the assembly ($v$) is $V_f = m/(\rho v)$, therefore:

$$v = \frac{m}{\rho V_f} \qquad (2)$$

$$v_0 = \frac{m}{\rho V_{f_0}} \quad (3)$$

while $V_{f0}$ is the initial value of $V_f$ when $P = 0$. Therefore Equation (1) can be modified to:

$$P = KE(V_f^3 - V_{f_0}^3) \quad (4)$$

In addition, for an ideal case that all the fibers are oriented randomly and distributed uniformly, the relationship between fiber area fraction $A_f$ and volume fraction is:

$$A_f = \frac{V_f}{2\pi}, ^3 \quad (5)$$

The whole resistance of the fabric sensor ($R$) with a resistive sensing fabric sandwiched between two conductive fabric electrodes can be regarded as the series connection of the bulk resistance of the resistive sensing fabric ($R_b$) and two contact resistances at the sensing fabric/electrode interfaces ($R_c$) [4, 5]:

$$R = 2R_c + R_b \quad (6)$$

It is found that the variation in $R_c$ is much more significant than that in $R_b$ at a normal pressure applied to the device, so $R_b$ can be regarded as a constant under pressure. Moreover, for the sandwich sensing structure with thin resistive sensing fabric, $R_b$ could be small enough to ignore in the equation. Therefore the response of the APPS is dominated by $R_c$ which is formed between the interfacial areas of the resistive fabric and the textile electrodes [6, 7].

In theory, the contact resistance $R_c$ can be calculated from the contact resistivity $\rho_c$ and the contact area $A_c$. $\rho_c$ is an intrinsic property of the interfacing materials, and can be defined as:

$$\rho_c = \lim_{A_c \to 0}(R_c \bullet A_c), ^{8\text{-}10} \quad (7)$$

Clearly for a given $\rho_c$, the contact resistance is inversely proportional to the contact area [8-10]:

$$R_c = \frac{\rho_c}{A_c} \quad (8)$$

And the resistance of the fabric sensor can be expressed as:

$$R = \frac{2\rho_c}{A_c} + R_b \quad (9)$$

At given pressure applied to the sensing fabric, the contacting area $A_c$ can be calculated as:

$$A_c = A \bullet A_f \quad (10)$$

Where A is the nominal area in contacting.

Considering the actual physics, a corrected parameter $A_r$ is introduced to Equation (10) to assure $P = 0$, $A_c = 0$:

$$A_c = A \bullet A_f + A_r \tag{11}$$

Noting $P = 0$, $A_c = 0$, $V_f = V_{f_0}$, there is

$$A_r = -\frac{AV_{f0}}{2\pi} \tag{12}$$

Replacing $A$, $A_f$ and

$$A_c = \frac{A}{2\pi} \bullet [(\frac{P}{KE} + V_{f_0}^3)^{\frac{1}{3}} - V_{f_0}] \tag{13}$$

Plugging (13) into (9):

$$R = \frac{4\pi\rho_c}{A \bullet [(\frac{P}{KE} + V_{f_0}^3)^{\frac{1}{3}} - V_{f_0}]} \tag{14}$$

Equation (14) can be simplified via Taylor expansion when $\frac{P}{KE} << 1$, i.e. the applied pressure is relatively low or the Young`s modulus is very large, as:

$$R = \frac{12\pi K \rho_c E V_{f_0}^2}{AP} \tag{15}$$

If the mechanical properties of the resistive sensing fabric differ from that of the fabric electrodes, the parameters $K$, $E$, and $V_{f0}$ in equation (15) can be replaced by the harmonic mean of the mechanical properties of the resistive sensing fabric and the conductive fabric electrodes separately [1]. As the harmonic means of two values are mainly determined by the smaller one, the parameters $K$, $E$ and $V_{f0}$ in equation (15) can be the smaller one between the resistive sensing fabric and the conductive fabric electrodes for simplifying the equation.

For unit device area, equation (15) can be simplified into:

$$R = \frac{k\rho_c E V_{f_0}^2}{P} \tag{16}$$

Whereas $k = 12\pi K$, and is a constant for given fabric.

References


1. J. Hu, *Structure and mechanics of woven fabrics*, Elsevier, 2004.
2. C. M. V. Wyk, *Journal of the Textile Institute Transactions*, 1946, **37**, T285-T292.
3. N. Pan, *Journal of Composite Materials*, 1994, **28**, 1500-1531.
4. M. Liu, X. Pu, C. Jiang, T. Liu, X. Huang, L. Chen, C. Du, J. Sun, W. Hu and Z. L. Wang, *Advanced Materials*, 2017, **29**, 1703700.
5. C. L. Choong, M. B. Shim, B. S. Lee, S. Jeon, D. S. Ko, T. H. Kang, J. Bae, S. H. Lee, K. E. Byun and J. Im, *Advanced materials*, 2014, **26**, 3451-3458.

6. N. Luo, W. Dai, C. Li, Z. Zhou, L. Lu, C. C. Poon, S. C. Chen, Y. Zhang and N. Zhao, *Advanced Functional Materials*, 2016, **26**, 1178-1187.
7. L. Pan, A. Chortos, G. Yu, Y. Wang, S. Isaacson, R. Allen, Y. Shi, R. Dauskardt and Z. Bao, *Nature communications*, 2014, **5**, 3002.
8. H. Berger, *Journal of the Electrochemical Society*, 1972, **119**, 507-514.
9. L. Kogut and K. Komvopoulos, *Journal of Applied Physics*, 2003, **94**, 3153-3162.
10. G. S. Marlow and M. B. Das, *Solid-State Electronics*, 1982, **25**, 91-94.